

# Distributionally Robust Optimal Power Flow with Contextual Information

Adrián Esteban-Pérez, Juan M. Morales\*

*Department of Applied Mathematics, University of Málaga, Málaga, 29071, Spain*

---

## Abstract

In this paper, we develop a distributionally robust chance-constrained formulation of the Optimal Power Flow problem (OPF) whereby the system operator can leverage contextual information. For this purpose, we exploit an ambiguity set based on probability trimmings and optimal transport through which the dispatch solution is protected against the incomplete knowledge of the relationship between the OPF uncertainties and the context that is conveyed by a sample of their joint probability distribution. We provide an exact reformulation of the proposed distributionally robust chance-constrained OPF problem under the popular conditional-value-at-risk approximation. By way of numerical experiments run on a modified IEEE-118 bus network with wind uncertainty, we show how the power system can substantially benefit from taking into account the well-known statistical dependence between the point forecast of wind power outputs and its associated prediction error. Furthermore, the experiments conducted also reveal that the distributional robustness conferred on the OPF solution by our probability-trimmings-based approach is superior to that bestowed by alternative approaches in terms of expected cost and system reliability.

---

\*Corresponding author

*Email address:* [adrianesteban@uma.es](mailto:adrianesteban@uma.es), [juan.morales@uma.es](mailto:juan.morales@uma.es) (Adrián Esteban-Pérez, Juan M. Morales)

*Keywords:* OR in Energy, Optimal Power Flow, Distributionally robust chance-constrained optimization, Wasserstein metric, Contextual information

---

## 1. Introduction

The Optimal Power Flow (OPF) is a fundamental problem in power system operations. Traditionally, the goal of the OPF problem is to minimize the cost of the power generation dispatch that supplies the electricity demand while complying with some physical and engineering constraints. The growing penetration of electricity generation sources such as wind and solar power, which are intrinsically uncertain, has led power system engineers to account for randomness in OPF analyses. Hence, the OPF is to be formulated today as an optimization problem *under uncertainty*.

A common way to cope with uncertainty in the constraints of an optimization problem and, in particular, of an OPF model is by way of the so-called *chance constraints*, which allow the modeler to impose the constraint satisfaction with a certain probability only. Accordingly, chance-constrained optimal power flow models (CC-OPF) have been developed to control the violation probability of, for instance, line and generation capacity limits. In particular, references [32], [16], [24] consider *joint* chance constraints, by which the system operator enforces that all constraints must simultaneously hold with a probability greater than or equal to  $1 - \epsilon$ , where  $\epsilon \in (0, 1)$  is a pre-fixed acceptable tolerance of dispatch infeasibility. This is opposed to *single* chance constraints, whereby the probability of constraint satisfaction is imposed on each constraint of the OPF separately. Although single chance constraints have been considered in the technical literature of CC-OPF models due to their attractive tractability properties (see, e.g., [35], [5], [20], [28] and references therein), satisfying all multiple individual constraints does not provide strong guarantees on the security of the entire power system, and leads to costly and over-conservative dispatch

solutions to achieve joint feasibility [24].

In any case, one of the main challenges in solving CC-OPF problems is that the underlying probability distribution of the random variables affecting the OPF constraints is generally unknown. In fact, in practice, only past historical observations of those variables are available to the system operator. Within this context, Distributionally Robust Optimization (DRO) has emerged as a versatile and powerful paradigm to tackle the ambiguity of the distribution of an optimization problem's random parameters. To this end, DRO considers a set of potential distributions for those parameters, namely, the so-called *ambiguity set* [27]. In the literature on DRO, there exist two distinct ways to specify an ambiguity set, either using statistical moments or probability metrics. The main drawback of using a *moment-based* DRO approach is that the available historical information is only used to estimate the moments of the true data-generating distribution and thus, if new samples of said distribution become available, but the moment estimates are not modified, the ambiguity set does not change. Alternatively, in *metric-based* DRO, the ambiguity set collects all potential distributions whose distance to a particular nominal distribution is lower than or equal to some pre-fixed value. Although there are different choices of probability metrics to construct the ambiguity set, the Wasserstein distance has received much attention within the power systems community. This is partly due to the performance guarantees provided by this distance (see, e.g., [22]) in contrast to the moment-based DRO approach.

Therefore, Distributionally Robust Chance-Constrained Optimal Power Flow (DRCC-OPF) models seek the optimal dispatch such that all the model constraints are satisfied with a pre-fixed confidence level for all the probability distributions within the ambiguity set built either by means of the Wasserstein metric ([1], [2], [8], [15], [12], [25], [26], [36]) or using moments ([17], [18], [19], [21], [29], [33]). In addition, the

system operator can not only tune the robustness of the resulting chance-constrained DRO model by adjusting the probability of constraint violation, but also, and very importantly, through the specificity degree of the ambiguity set. In this regard, some previous approaches have focused on producing more meaningful ambiguity sets by incorporating structural information on the underlying true probability distribution (see, e.g., [1], [17], [18], [19]).

Unfortunately, the consideration of *joint* chance constraints in a DRO framework ([13], [34]) renders an intractable optimization problem in general. For this reason, researchers have considered DRO-OPF models based on the well-known conservative, but far more tractable approximation given by the concept of *conditional-value-at-risk* (**CVaR**), see, for example, [1], [8], [12], [15], [25], [26] and references therein. The authors in [7] show that the **CVaR** offers a tight convex approximation of the chance constraints under the DRO framework, which justifies its popularity. On top of that, by way of **CVaR**-based chance-constraints, the power system operator can control not only the violation probability, but also the violation magnitude, which may be important from the standpoint of power system operations.

The present work follows a path similar to that undertaken by [1], [17], [18], and [19]: Our aim is also to leverage a sharper ambiguity set, but, for the first time to our knowledge, by exploiting some side/contextual information. This information (also known as *features* or *attributes*) is related to outcomes of random variables that may have predictive power on the OPF's uncertainties. More specifically, in the work we present here, we exploit the contextual information provided by the *point forecasts* of those uncertainties. Indeed, it is well known in the energy forecasting community that the power forecast error of a wind farm highly depends on the wind power forecast itself [6, 11]. Within the context of DRCC-OPF, this means that the wind power point forecast constitutes valuable information to build a proper ambiguity set for

the wind power forecast error.

The main contributions of this work are thus:

1. We provide a formulation of the DC-OPF problem with *joint* chance constraints as a *conditional stochastic program*, in which both the expected cost of the power dispatch and the chance constraints are conditioned on some contextual information, in particular, the point forecasts of the OPF's uncertainties.
2. To tackle the resulting conditional stochastic program, we propose an entirely data-driven and non-parametric DRO approach, in which no assumption on the relationship between the context and the OPF's uncertainties (i.e., the point forecasts and their error in our case) is made. Furthermore, the proposed DRO approach enjoys performance guarantees based on the results in [9].
3. We derive a tractable approximation and reformulation of the proposed DRCC-OPF using the Conditional Value at Risk.
4. Finally, by way of numerical experiments in which we compare our DRCC-OPF formulation with other sensible approaches, we show that exploiting the contextual information provided by the wind power point forecasts allows identifying dispatch solutions with a better trade-off between expected cost and system reliability.

The remainder of this paper is organized as follows. Section 2 introduces the mathematical formulation of the distributionally robust joint chance-constrained DC-OPF problem with contextual information that we propose. Then, Section 3 provides a tractable reformulation of the distributionally robust joint chance constraints under the well-known CVaR approximation, while Section 4 focuses on reformulating the worst-case expected cost in a manageable way. Results from numerical experiments

are presented and discussed in Section 5. Finally, Section 6 concludes the paper with some final remarks. The manuscript is also accompanied by supplementary material in the form of appendices with the main notation used throughout the main text, supportive mathematical concepts and optimization models, proofs of theoretical results, and additional numerical experiments.

## 2. DC-OPF under uncertainty: Mathematical Formulation

Consider a power system with a set  $\mathcal{L}$  of transmission lines, a set  $B$  of buses,  $N_W$  wind power plants, and  $N_G$  generators. For ease of formulation, power loads are assumed to be deterministic. Next we introduce each of the main components of the DC-OPF problem. The reader is referred to Appendix A for a complete list of the notation used throughout this paper.

1. *Wind power plants.* For each wind power plant  $m \in \{1, \dots, N_W\}$ , the random power output is modeled as  $f_m + \omega_m$ , where  $f_m$  is the predicted power output and  $\omega_m$  is the (random) wind forecast error at wind power plant  $m$ . We denote the system-wise aggregate wind power forecast error as  $\Omega$ , i.e.,  $\Omega := \sum_{m=1}^{N_W} \omega_m$ .
2. *Generators:* For each  $j = 1, \dots, N_G$ , the actual power output of generator  $j$ ,  $g_j(\boldsymbol{\omega})$ , is expressed as the sum of the scheduled generation,  $g_j$ , and the (random) adjusted power  $r_j(\boldsymbol{\omega})$  (also known as *deployed reserve*). As customary, we assume an affine control policy to counterbalance the wind forecast errors by deploying generators' reserves [5], that is,

$$g_j(\boldsymbol{\omega}) := g_j + r_j(\boldsymbol{\omega}) = g_j - \beta_j \Omega, \quad \forall j \leq N_G \quad (1)$$

where  $\beta_j$  is the participation factor of generator  $j$ .

3. *Power balance.* The total power generation must equal the total system demand, that is,

$$\sum_{j=1}^{N_G} g_j(\boldsymbol{\omega}) + \sum_{m=1}^{N_w} (f_m + \omega_m) = \sum_{b \in B} L_b \quad (2)$$

where  $L_b$  denotes the load at bus  $b$ . Using (1), Eq. (2) is equivalent to:

$$\sum_{j=1}^{N_G} g_j + \sum_{m=1}^{N_w} f_m = \sum_{b \in B} L_b \quad (3)$$

$$\sum_{j=1}^{N_G} \beta_j = 1 \quad (4)$$

which guarantee the power balance both in the dispatch and the real-time stages, respectively.

4. *Power flows.* The power flow through line  $\ell \in \mathcal{L}$  is given as a linear function of the nodal power injections:

$$D_\ell(\mathbf{g}(\boldsymbol{\omega}) + \mathbf{f} + \boldsymbol{\omega} - \mathbf{L}) \quad (5)$$

where  $D_\ell$  denotes the row of the matrix  $D$  given by the DC power transfer distribution factors corresponding to line  $\ell$  [31].

5. *OPF Constraints.* The following constraints limit the production of generators to their power capacity:

$$g_j^{\min} \leq g_j - \beta_j \Omega, \quad \forall j \leq N_G \quad (6)$$

$$g_j - \beta_j \Omega \leq g_j^{\max}, \quad \forall j \leq N_G \quad (7)$$

where  $g_j^{\min}, g_j^{\max}$  are the minimum and maximum power output of generator  $j$ , respectively. The following constraints determine the provision of reserve capacities:

$$-r_j^D \leq -\beta_j \Omega, \quad \forall j \leq N_G \quad (8)$$

$$-\beta_j \Omega \leq r_j^U, \quad \forall j \leq N_G \quad (9)$$

with  $r_j^D, r_j^U$  being the downward and upward reserve capacity provided by generator  $j$ , in that order.

Naturally, the following physical constraints, which link the generation dispatches and the provision of reserve capacities, must hold:

$$g_j + r_j^U \leq g_j^{\max}, \quad \forall j \leq N_G \quad (10)$$

$$g_j - r_j^D \geq g_j^{\min}, \quad \forall j \leq N_G \quad (11)$$

Finally, the constraints

$$-\text{Cap}_\ell \leq D_\ell(\mathbf{g}(\boldsymbol{\omega}) + \mathbf{f} + \boldsymbol{\omega} - \mathbf{L}) \leq \text{Cap}_\ell, \quad \forall \ell \in \mathcal{L} \quad (12)$$

enforce the transmission capacity limits based on the DC power flow approximation, where  $\text{Cap}_\ell$  denotes the capacity of transmission line  $\ell \in \mathcal{L}$ .

6. *Cost function.* This is given by the sum of the (random) total generation cost and the (deterministic) cost of providing up- and down-reserve capacities:

$$\sum_{j=1}^{N_G} C_j(g_j(\boldsymbol{\omega})) + \sum_{j=1}^{N_G} (c_j^D r_j^D + c_j^U r_j^U) \quad (13)$$

$C_j(\cdot)$  is the cost function of generator  $j$ , which is given by a convex piecewise linear cost function with  $S_j$  pieces/blocks, i.e.,

$$C_j(x) := \max_{s=1, \dots, S_j} \{m_s^j x + n_s^j\} \quad (14)$$

where  $m_s^j, n_s^j$  stands for the slope and the intercept of the  $s$ -th piece for generator  $j$ , respectively.



2.1. *Dealing with uncertainty in the DC-OPF problem: Joint chance constraints, Distributionally Robust Optimization and contextual information*

In practice, it is often the case that the random vector of forecast errors  $\boldsymbol{\omega}$  shows some statistical dependence on some features/covariates, which we can model, in general, by some random vector  $\mathbf{z}$ . In fact, the forecast wind power output  $\mathbf{f}$  serves in itself as an obvious explanatory random vector for the subsequent forecast error  $\boldsymbol{\omega}$ . In this approach, we want to exploit that statistical dependence to identify a better power generation dispatch and provision of reserve capacity.

Let  $\mathbf{z} := (z_1, \dots, z_{N_W})$  be the random vector modeling the features and let  $\mathbb{Q}$  be the probability measure of the joint distribution of  $\mathbf{z}$  and  $\boldsymbol{\omega}$ , which is supported on  $\tilde{\Xi}$ . Given the array of forecast wind power outputs,  $\mathbf{f} := (f_1, \dots, f_{N_W})$ , our aim is to solve the following conditional stochastic problem:

$$(P_1^*) \min_{\mathbf{x} \in X} \mathbb{E}_{\mathbb{Q}} \left[ \sum_{j=1}^{N_G} C_j(g_j(\boldsymbol{\omega})) + \sum_{j=1}^{N_G} (c_j^D r_j^D + c_j^U r_j^U) \mid (\mathbf{z}, \boldsymbol{\omega}) \in \tilde{\Xi} \right] \quad (15)$$

$$\text{s.t. } \mathbb{Q} \left( (6) - (9), (12) \mid (\mathbf{z}, \boldsymbol{\omega}) \in \tilde{\Xi} \right) \geq 1 - \epsilon \quad (16)$$

where  $\mathbf{x} := (\mathbf{g}, \boldsymbol{\beta}, \mathbf{r}^D, \mathbf{r}^U)$  stands for the vector of decision variables,  $X$  comprises the constraints (4), (3), (10) and (11); and  $(\mathbf{z}, \boldsymbol{\omega}) \in \tilde{\Xi}$  stands for the event  $(z_1 = f_1, \dots, z_{N_W} = f_{N_W}; \boldsymbol{\omega} \in \tilde{\Xi}_{\boldsymbol{\omega}})$ , with  $\tilde{\Xi}_{\boldsymbol{\omega}}$  being the support of  $\boldsymbol{\omega}$  conditional on  $\tilde{\Xi}$ . Due to the physical nature of the problem,  $\tilde{\Xi}_{\boldsymbol{\omega}}$  is the hypercube  $\prod_{m=1}^{N_W} [-f_m, \bar{C}_m - f_m]$ , where  $\bar{C}_m$  represents the capacity of wind farm  $m$ . Equation (16) constitutes the joint chance constraints, which establish a tolerance  $\epsilon$  in terms of the joint violation probability of the OPF constraints under  $\mathbb{Q}$  given the context  $\tilde{\Xi}$ .

The optimal solution to  $(P_1^*)$  (namely, the power generation dispatch and the reserve capacity provision) is, therefore, parametrized on the predicted wind power outputs  $f_1, \dots, f_{N_W}$ . In fact,  $(P_1^*)$  can be equivalently recast using the conditional

distribution of  $\mathbb{Q}$  given  $\mathbf{z} = \mathbf{f}$ ,  $\mathbb{Q}_{\boldsymbol{\omega}/\mathbf{z}=\mathbf{f}}$ , as follows:

$$(P_2^*) \min_{\mathbf{x} \in X} \mathbb{E}_{\mathbb{Q}_{\boldsymbol{\omega}/\mathbf{z}=\mathbf{f}}} \left[ \sum_{j=1}^{N_G} C_j(g_j(\boldsymbol{\omega})) + \sum_{j=1}^{N_G} (c_j^D r_j^D + c_j^U r_j^U) \right] \quad (17)$$

$$\text{s.t. } \mathbb{Q}_{\boldsymbol{\omega}/\mathbf{z}=\mathbf{f}}((6) - (9), (12)) \geq 1 - \epsilon \quad (18)$$

In real life, however, neither the joint distribution  $\mathbb{Q}$ , nor the conditional one  $\mathbb{Q}_{\boldsymbol{\omega}/\mathbf{z}=\mathbf{f}}$ , are known. The system operator only has access to a finite set of samples of size  $N$  (i.e. the training set) of the true joint distribution  $\mathbb{Q}$ , which we denote as  $\widehat{\Xi}_\omega^N := \{(\widehat{\mathbf{z}}_i, \boldsymbol{\omega}_i)\}_{i=1}^N$ . In our context,  $\widehat{\Xi}_\omega^N$  is made up of  $N$  past observations of the predicted wind power outputs and their associated errors. Hence, the system operator needs to infer or construct a proxy of  $\mathbb{Q}_{\boldsymbol{\omega}/\mathbf{z}=\mathbf{f}}$  from the sample  $\widehat{\Xi}_\omega^N$ , so that this proxy can be used as an input for problem  $(P_2^*)$ . However, the limited information that  $\widehat{\Xi}_\omega^N$  conveys on  $\mathbb{Q}_{\boldsymbol{\omega}/\mathbf{z}=\mathbf{f}}$  makes this inference process ambiguous, and as such, we propose employing Distributionally Robust Optimization to protect the system operator's decision against this ambiguity. To this end, we will solve the following chance-constrained DRO DC-OPF problem in replacement of  $(P_2^*)$ :

$$(CC - DRO) \min_{\mathbf{x} \in X} \sup_{Q \in \widehat{\mathcal{U}}} \mathbb{E}_Q \left[ \sum_{j=1}^{N_G} C_j(g_j(\boldsymbol{\omega})) + \sum_{j=1}^{N_G} (c_j^D r_j^D + c_j^U r_j^U) \right] \quad (19)$$

$$\text{s.t. } \inf_{Q \in \widehat{\mathcal{U}}} Q((6) - (9), (12)) \geq 1 - \epsilon \quad (20)$$

where  $\widehat{\mathcal{U}}$  stands for an ambiguity set for the true conditional distribution  $\mathbb{Q}_{\boldsymbol{\omega}/\mathbf{z}=\mathbf{f}}$ .

Here we will use the ambiguity set based on probability trimmings and optimal transport introduced in [9], which allows us to exploit the side information within a DRO framework in a fully data-driven sense. Our ambiguity set is thus defined as follows:

**Definition 1** (Ambiguity set based on probability trimmings). Assume that  $\mathbb{Q} \in \mathcal{P}_p(\Xi)$ ,  $\alpha > 0$ , and consider the set  $\mathcal{R}_{1-\alpha}(\widehat{\mathbb{Q}}_N)$  of  $(1 - \alpha)$ -trimmings of the empirical joint distribution  $\widehat{\mathbb{Q}}_N := \frac{1}{N} \sum_{i=1}^N \delta_{(\widehat{\mathbf{z}}_i, \boldsymbol{\omega}_i)}$ . If  $\tilde{\rho} \geq \underline{\epsilon}_{N\alpha}^p$  (i.e., the  $p$ -th power of the minimum transportation budget), then the ambiguity set based on trimmings,  $\widehat{\mathcal{U}}_N(\alpha, \tilde{\rho})$ , is defined as the set of all distributions  $Q_{\Xi}$  supported on  $\tilde{\Xi}$  such that  $\mathcal{W}_p^p(\mathcal{R}_{1-\alpha}(\widehat{\mathbb{Q}}_N), Q_{\Xi}) \leq \tilde{\rho}$ , with  $\mathcal{W}_p$  being the  $p$ -Wasserstein distance.

Definitions of a trimming set of a probability distribution and of the minimum transportation budget  $\underline{\epsilon}_{N\alpha}$  can be found in Appendix B. Further technical information on the ambiguity set  $\widehat{\mathcal{U}}_N(\alpha, \tilde{\rho})$  can be obtained from [9].

Finally, the chance-constrained DRO OPF model we propose is written as follows:

$$\min_{\mathbf{x} \in X} \sup_{Q_{\Xi} \in \widehat{\mathcal{U}}_N(\alpha, \tilde{\rho})} \mathbb{E}_{Q_{\Xi}} \left[ \sum_{j=1}^{N_G} C_j(g_j(\boldsymbol{\omega})) + \sum_{j=1}^{N_G} (c_j^D r_j^D + c_j^U r_j^U) \right] \quad (21)$$

$$\text{s.t.} \quad \inf_{Q_{\Xi} \in \widehat{\mathcal{U}}_N(\alpha, \tilde{\rho})} Q_{\Xi}((6) - (9), (12)) \geq 1 - \epsilon \quad (22)$$

We remark that, in order to account for side information in a DRO framework, the authors in [4] propose an ambiguity set  $\widehat{\mathcal{U}}$  different to the one based on probability trimmings (i.e.,  $\widehat{\mathcal{U}}_N(\alpha, \tilde{\rho})$ ) that we advocate here. More specifically, the ambiguity set they suggest is a Wasserstein ball centered at the discrete distribution that results from projecting onto the conditional support  $\tilde{\Xi}$  the  $K$  data points from the sample  $\widehat{\Xi}_{\boldsymbol{\omega}}^N$  that are the closest to  $\tilde{\Xi}$ . In Appendix E, we use an example based on a small three-node system to illustrate that our trimmings-based ambiguity set generally delivers better dispatch solutions in terms of expected cost and system reliability than the one introduced in [4] for the DC-OPF problem under uncertainty.

In the next section, we introduce a tractable and conservative approximation of the distributionally robust joint chance constraints (22) using the notion of Conditional

Value at Risk (CVaR). The use of the CVaR to this end in the context of chance-constrained distributionally robust OPF is very popular in the technical literature (see, for example, the recent publications [15] and [25]).

### 3. A tractable and conservative CVaR-based approximation of the distributionally robust joint chance constraints

The distributionally robust joint chance constraints (22) can be written equivalently as the following distributionally robust single chance constraint:

$$\inf_{Q_{\Xi} \in \widehat{\mathcal{U}}_N(\alpha, \tilde{\rho})} Q_{\Xi} \left( \max_{k \leq K} \phi_k(\mathbf{x}, \boldsymbol{\omega}) \leq 0 \right) \geq 1 - \epsilon \quad (23)$$

where functions  $\phi_k(\mathbf{x}, \boldsymbol{\omega})$ ,  $k \leq K$ , represent the OPF constraints introduced in Section 2 expressed as inequalities lower than or equal to zero.

In this paper, in lieu of (23), we consider the following tractable (convex) approximation:

$$\sup_{Q_{\Xi} \in \widehat{\mathcal{U}}_N(\alpha, \tilde{\rho})} Q_{\Xi} - \mathbf{CVaR}_{\epsilon} \left( \max_{k \leq K} \phi_k(\mathbf{x}, \boldsymbol{\omega}) \right) \leq 0 \quad (24)$$

which is, in addition, conservative, because (24) implies (23).

We work with  $p = 1$ , i.e., with the 1-Wasserstein metric (and hence the 1-norm) to construct the ambiguity set based on trimmings  $\widehat{\mathcal{U}}_N(\alpha, \tilde{\rho})$ , because it leads to a linear program that can be solved by off-the-self optimization software.

Constraint (24) can be equivalently reformulated as follows [25], [30]:

$$\inf_{\tau \in \mathbb{R}} \left\{ \tau + \frac{1}{\epsilon} \sup_{Q_{\Xi} \in \widehat{\mathcal{U}}_N(\alpha, \tilde{\rho})} \mathbb{E}_{Q_{\Xi}} \left[ \left( \max_{k \leq K} \phi_k(\mathbf{x}, \boldsymbol{\omega}) - \tau \right)^+ \right] \right\} \leq 0 \quad (25)$$

The next proposition states a tractable reformulation of (25). For ease of exposition, we first need to recast function  $(\max_{k \leq K} \phi_k(\mathbf{x}, \boldsymbol{\omega}) - \tau)^+$  as

$$\left( \max_{k \leq K} \phi_k(\mathbf{x}, \boldsymbol{\omega}) - \tau \right)^+ := \max_{k \leq K+1} \langle \mathbf{a}_{1k}, \boldsymbol{\omega} \rangle + a_{2k} \quad (26)$$

where for  $k = K + 1$ , we have  $\mathbf{a}_{1K+1} = \mathbf{0}$  and  $a_{2K+1} = 0$ .

**Proposition 1** (Reformulation of the **CVaR**-based distributionally robust joint chance constraints). *Set  $\alpha > 0$  and take the 1-Wasserstein metric ( $p = 1$ ) with the 1-norm. Then, for any value of  $\tilde{\rho} \geq \epsilon_{N\alpha}$ , the **CVaR**-based distributionally robust joint chance constraints defined by (24) can be equivalently reformulated as follows:*

$$\inf_{\tau \in \mathbb{R}, \lambda_2 \geq 0, \mu_i \geq 0, \theta_2 \in \mathbb{R}} \left\{ \tau + \frac{1}{\epsilon} \left[ \lambda_2 \tilde{\rho} + \theta_2 + \frac{1}{N\alpha} \sum_{i=1}^N \mu_i \right] \right\} \leq 0 \quad (27a)$$

$$\begin{aligned} \text{s.t. } & \mu_i + \theta_2 + \lambda_2 \|\mathbf{z}^* - \hat{\mathbf{z}}_i\|_1 \geq a_{2k} + S_{\tilde{\Xi}_\omega}(\mathbf{v}_{ik}) \\ & - \langle \mathbf{z}_{ik}, \hat{\boldsymbol{\omega}}_i \rangle, \forall i \leq N, \forall k \leq K + 1 \end{aligned} \quad (27b)$$

$$\mathbf{z}_{ik} - \mathbf{v}_{ik} = -\mathbf{a}_{1k}, \forall i \leq N, \forall k \leq K + 1 \quad (27c)$$

$$\|\mathbf{z}_{ik}\|_\infty \leq \lambda_2, \forall i \leq N, \forall k \leq K + 1 \quad (27d)$$

where  $S_{\tilde{\Xi}_\omega}(\cdot)$  stands for the support function of  $\tilde{\Xi}_\omega$  and  $\langle \cdot, \cdot \rangle$  represents the dot product (see Appendix A).

*Proof:* The proof of this proposition is a direct application of [9, Theorem 1], after noticing that the inner supremum in constraint (25) involves a maximum of linear functions (because each function  $\phi_k(\mathbf{x}, \boldsymbol{\omega})$  is linear on the uncertainty  $\boldsymbol{\omega}$ ).

Once we have reformulated the **CVaR**-based distributionally robust joint chance constraint (24), we only need to reformulate the DRO problem defined by the inner supremum in (21). Since this requires a careful and independent analysis, we consider it in the following section.

#### 4. An exact tractable reformulation of the worst-case expected cost

In what follows, we provide an exact and tractable reformulation of the objective function (21) as a continuous linear program.

The term

$$\sum_{j=1}^{N_G} C_j(g_j(\boldsymbol{\omega})) = \sum_{j=1}^{N_G} \max_{s=1, \dots, S_j} \left\{ m_s^j [g_j - \beta_j \Omega] + n_s^j \right\} \quad (28)$$

is a sum of a maximum of *univariate* linear functions in terms of  $\Omega$ , which is, moreover, convex in  $\Omega$ . This observation is key to reformulating (21) in a tractable way. In fact, the ambiguity set  $\widehat{\mathcal{U}}_N(\alpha, \tilde{\rho})$  for the worst-case probability distribution in the inner supremum of (21) can be equivalently replaced with the following one, which is also expressed in terms of  $\Omega$  only:

$$\widehat{\mathcal{U}}_N^\Omega(\alpha, \rho) := \{P_{\tilde{\Xi}_\Omega} : \mathcal{W}_p^p(\mathcal{R}_{1-\alpha}(\widehat{\mathbb{P}}_N), P_{\tilde{\Xi}_\Omega}) \leq \rho, P_{\tilde{\Xi}_\Omega}(\tilde{\Xi}_\Omega) = 1\} \quad (29)$$

where  $\widehat{\mathbb{P}}_N := \frac{1}{N} \sum_{i=1}^N \delta_{(\widehat{\mathbf{z}}_i, \widehat{\Omega}_i)}$  is the empirical distribution supported on the samples  $(\widehat{\mathbf{z}}, \widehat{\Omega}_i), i = 1, \dots, N$ ; and  $\tilde{\Xi}_\Omega$  stands for the event

$$(\mathbf{z} = \mathbf{f}; \Omega \in [\underline{\Omega}, \overline{\Omega}]), \text{ with } [\underline{\Omega}, \overline{\Omega}] = \left[ -\sum_{m=1}^{N_W} f_m, \sum_{m=1}^{N_W} (\overline{C}_m - f_m) \right]$$

The interval  $[\underline{\Omega}, \overline{\Omega}]$  is the conditional support for the random variable  $\Omega$  (that is, the support set for the system-wise aggregate wind power forecast error, given the predicted power outputs of the wind farms). Essentially, what we have done above is to map the original probability space for the random vector  $(\mathbf{z}, \boldsymbol{\omega})$  onto a new probability space for the random vector  $(\mathbf{z}, \Omega)$  by the projection  $\Omega = \sum_{m=1}^{N_W} \omega_m$ , which leaves the objective cost function unaltered. In doing so, the inner supremum in (21) can be fully recast in terms of  $\Omega$  only as follows:

$$\sup_{P_{\tilde{\Xi}_\Omega} \in \widehat{\mathcal{U}}_N^\Omega(\alpha, \tilde{\rho})} \mathbb{E}_{P_{\tilde{\Xi}_\Omega}} \left[ \sum_{j=1}^{N_G} \max_{s=1, \dots, S_j} \left\{ m_s^j [g_j - \beta_j \Omega] + n_s^j \right\} + \sum_{j=1}^{N_G} (c_j^D r_j^D + c_j^U r_j^U) \right] \quad (30)$$

The proposition below presents a tractable reformulation of (30) as a continuous linear program.

**Proposition 2** (LP reduction of the worst-case expected cost). *Set  $\alpha > 0$  and assume that  $p = 1$  and that  $\|(\mathbf{z}, \Omega)\| := \|\mathbf{z}\| + |\Omega|$  for some norm  $\|\cdot\|$  in  $\mathbb{R}^{d_{\mathbf{z}}}$ . Then, for any value of  $\tilde{\rho} \geq \underline{\epsilon}_{N\alpha}$ , the DRO problem defined by (30) can be reformulated as the following continuous linear program:*

$$\inf_{\lambda \geq 0; \bar{\mu}_i, \forall i \leq N; \theta \in \mathbb{R}} \lambda \tilde{\rho} + \theta + \frac{1}{N\alpha} \sum_{i=1}^N \bar{\mu}_i + \sum_{j=1}^{N_G} (c_j^D r_j^D + c_j^U r_j^U) \quad (31a)$$

$$\text{s.t. } \bar{\mu}_i + \theta + \lambda \|\mathbf{z}^* - \hat{\mathbf{z}}_i\| \geq t_i, \forall i \leq N \quad (31b)$$

$$t_i \geq \sum_{j=1}^{N_G} \underline{t}_{ij} - \lambda(\underline{\Omega} - \hat{\Omega}_i), \forall i \in \underline{I} \quad (31c)$$

$$t_i \geq \sum_{j=1}^{N_G} \bar{t}_{ij} - \lambda(\bar{\Omega} - \hat{\Omega}_i), \forall i \in \underline{I} \quad (31d)$$

$$t_i \geq \sum_{j=1}^{N_G} \underline{t}_{ij} + \lambda(\underline{\Omega} - \hat{\Omega}_i), \forall i \in \bar{I} \quad (31e)$$

$$t_i \geq \sum_{j=1}^{N_G} \bar{t}_{ij} + \lambda(\bar{\Omega} - \hat{\Omega}_i), \forall i \in \bar{I} \quad (31f)$$

$$t_i \geq \sum_{j=1}^{N_G} \bar{t}_{ij} - \lambda(\bar{\Omega} - \hat{\Omega}_i), \forall i \in I \quad (31g)$$

$$t_i \geq \sum_{j=1}^{N_G} \underline{t}_{ij} + \lambda(\underline{\Omega} - \hat{\Omega}_i), \forall i \in I \quad (31h)$$

$$t_i \geq \sum_{j=1}^{N_G} \hat{t}_{ij}, \forall i \in I \quad (31i)$$

$$\bar{\mu}_i \geq 0, \forall i \leq N \quad (31j)$$

$$\underline{t}_{ij} \geq m_s^j [g_j - \beta_j \underline{\Omega}] + n_s^j, \forall i \leq N, \forall j \leq N_G, \forall s \leq S_j \quad (31k)$$

$$\bar{t}_{ij} \geq m_s^j [g_j - \beta_j \bar{\Omega}] + n_s^j, \forall i \leq N, \forall j \leq N_G, \forall s \leq S_j \quad (31l)$$

$$\hat{t}_{ij} \geq m_s^j [g_j - \beta_j \hat{\Omega}_i] + n_s^j, \forall i \leq N, \forall j \leq N_G, \forall s \leq S_j \quad (31m)$$

where  $\underline{I} := \{i \in \{1, \dots, N\} : \hat{\Omega}_i < \underline{\Omega}\}$ ,  $I := \{i \in \{1, \dots, N\} : \hat{\Omega}_i \in [\underline{\Omega}, \bar{\Omega}]\}$ , and  $\bar{I} := \{i \in \{1, \dots, N\} : \hat{\Omega}_i > \bar{\Omega}\}$ .

*Proof:* See Appendix C.

## 5. Numerical results

In this section, we present and discuss results from a series of numerical experiments that have been run on a modified version of the IEEE 118-bus system considered in [15]. All the data and codes needed to reproduce those experiments are available for download in the GITHUB repository [10]. The experiments have been carried out on a Linux-based server using up to 600 CPUs running in parallel, each clocking at 2.6 GHz with 60 GB of RAM. We have employed CPLEX 20.1.0 under Pyomo 5.2 to solve the associated continuous linear programs. In addition, we have set the CPLEX parameter `preprocessing_dual` to 1.

We solve the CC-DRO OPF problem (19)–(22) using the **CVaR**-based approximation stated above, but with different ambiguity sets, namely: (i) The ambiguity set based on probability trimmings, introduced in this paper, which we refer to as DROTRIMM; and (ii) a Wasserstein ball centered at the finite discrete distribution that results from projecting the  $N$  samples in  $\hat{\Xi}_\omega^N$  onto the conditional support  $\tilde{\Xi}$ . We denote this latter approach as PDROW. Importantly, we can interpret PDROW as a DRO model that partially ignores the contextual information, since the center of the Wasserstein ball it uses is made up of *all* past samples of wind power forecast errors (regardless of the current wind power point predictions), albeit adjusted to fit in the conditional support. Roughly speaking, DROTRIMM also works with all the past  $N$  samples of wind power forecast errors, but only those that lead to the worst-case conditional distribution of the prediction errors are moved onto the conditional support.



However, this movement must entail a transportation cost smaller than or equal to a given budget  $\rho$  and the computation of that cost is directly contingent on the current context (that is, the current wind power point forecasts).

The training data consist of a set of pairs  $\{(\hat{\mathbf{z}}_i, \hat{\boldsymbol{\omega}}_i)\}_{i=1}^N$ , from which we can directly obtain the collection of pairs  $\{(\hat{\mathbf{z}}_i, \hat{\Omega}_i)\}_{i=1}^N$ , where  $\hat{\Omega}_i := \sum_{m=1}^{N_W} \hat{\omega}_{i,m}$ . For ease of computation and to simplify the analysis below, we have considered the same radius or transportation budget for the two ambiguity sets in both the objective and the chance constraints of the DRO OPF problem.

### 5.1. Evaluation of the out-of-sample performance via re-optimization

Given a context (in the form of point forecasts of the power outputs of the wind farms), a training dataset, and a robustness parameter  $\rho$ , each method  $m$  (either PDROW or DROTRIMM in our case) provides a forward generation dispatch and reserve capacity provision  $\mathbf{y}^m := (\mathbf{g}, \mathbf{r}^D, \mathbf{r}^U)$ . To evaluate the actual or out-of-sample performance of that  $\mathbf{y}^m$ , we draw a sample of wind power forecast errors  $\hat{\boldsymbol{\omega}}_j$  from a validation dataset, and the vector of recourse variables  $\mathbf{r}$  (that is, the real-time power adjustments) is computed by solving the deterministic optimal power flow available in Appendix D. In this deterministic OPF problem, wind spillage (with a cost equal to 0) and involuntary load curtailment (with a cost equal to \$500/MWh) are considered as feasible recourse actions, aside from the deployment of reserves by generators. In this way, the *out-of-sample performance* of a method  $m$ , which produces the forward dispatch  $\mathbf{y}^m$ ,  $J(\mathbf{y}^m)$ , is computed by the empirical out-of-sample cost over the validation set formed by a certain number of samples of  $\mathbb{Q}_{\boldsymbol{\omega}/\mathbf{z}=\mathbf{f}}$ . In addition, in order to measure the *reliability* of a solution (that is, if  $\mathbf{y}^m$  is feasible or not in real time), the *violation probability* is estimated over the validation set.

## 5.2. A 118-bus case study

As previously mentioned, we consider a modified version of the IEEE 118-bus system used in [15]. The system includes 54 conventional generators and four wind power plants that we have added and placed at buses 16, 37, 83 and 55. In addition, the piecewise linear cost functions of all generators are comprised of three pieces or blocks. All the data pertaining to the network, generators, and transmission lines are available at the GITHUB repository [10].

We analyze two scenarios, which differ in the level of wind power penetration in the system. Below we explain how we have generated samples for the joint distribution of the wind power forecast and its error at each wind power plant. The so generated samples are also available online at the GITHUB repository [10]:

1. Let  $\tilde{f}_m$  be the per-unit point forecast of the power output at wind plant  $m \in \{1, \dots, N_W\}$ . The samples have been taken from a collection of 16 801 p.u. wind power data recorded in several zones and made available by the Global Energy Forecasting Competition 2014 [14]. We have selected zones 1, 10, 3 and 5 of the aforementioned dataset and assigned them to the four wind power plants located at buses 16, 37, 83 and 55, respectively.
2. For each wind farm  $m$ , we have assumed that the (nominal, normalized) random variable  $W_m$ , which represents the nominal actual power generated at wind plant  $m$ , follows a Beta distribution with mean  $\tilde{f}_m$  and standard deviation  $\sigma$ . This standard deviation depends on both physical parameters and the quality of the forecasting model, following the model proposed in [11]. For simplicity, in all numerical experiments, given  $\tilde{f}_m$ , we determine  $\sigma$  as the value of the following function  $\sigma(\tilde{f}_m) := 0.2\tilde{f}_m + 0.02$ , empirically obtained in [11] for the case of a lead time of six hours. Therefore, the actual wind power production, and hence,

the forecast error are conditional on the forecast power output issued. More specifically, the forecast error is given as the difference of a realization  $\widehat{W}_m$  of the r.v.  $W_m \sim \text{Beta}(A, B)$  and the point forecast  $\tilde{f}_m$ , where  $A, B > 0$  are the solution (if it exists) of the following system of non-linear equations:

$$\tilde{f}_m = \frac{A}{A+B} \quad (32a)$$

$$\sigma^2(\tilde{f}_m) = \frac{AB}{(A+B)^2(A+B+1)} \quad (32b)$$

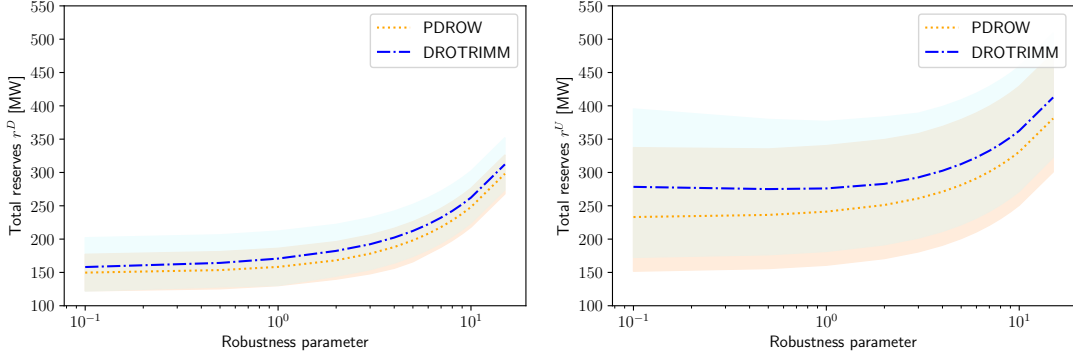
To ensure that this non-linear system of equations has a solution, the samples  $\tilde{f}_m$  from the dataset that are less than or equal to 0.05 p.u. are set to 0.05, and the ones greater than or equal to 0.95 p.u. are set to 0.95. Thus, for each wind power plant, the per-unit point forecast lies in the interval  $[0.05, 0.95]$ .

3. Finally, to work with MW, we multiply the per-unit realized power output and the point prediction  $\tilde{f}_m$  by the wind plant capacity  $\bar{C}_m$ , thus getting a pair of predicted power output and its error  $(\bar{C}_m \tilde{f}_m, \bar{C}_m (\widehat{W}_m - \tilde{f}_m))$  for wind farm  $m$ .

The validation set used to compute the out-of-sample performance of a data-driven solution via re-optimization is constructed by drawing 1000 samples from the wind-power-data generating model based on the beta distribution presented above. This validation set constitutes a discrete approximation of the forecast error distribution conditional on a given context, which will be specified later. Also, for DROTRIMM, we have set  $\alpha_N := K_N/N$  where  $K_N := \lfloor N^{0.9} \rfloor$ . This choice is consistent with the theoretical results included in [9].

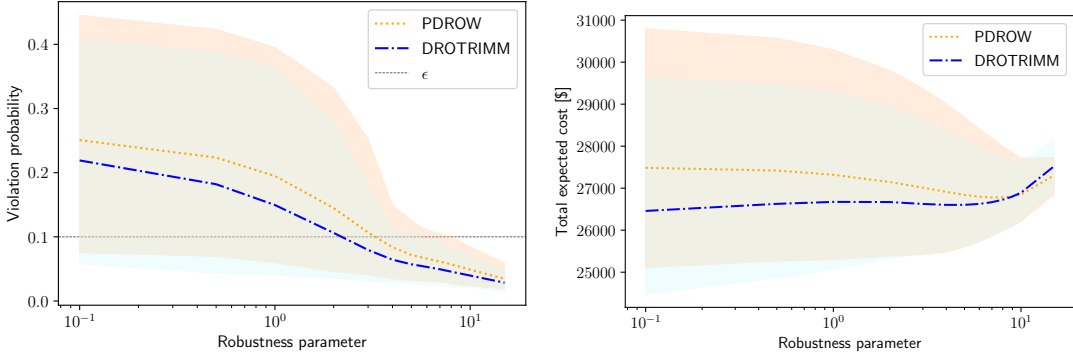
### 5.2.1. Medium wind penetration case

In this case, all four wind farms in the system have a capacity of 400 MW and the context is given by  $\mathbf{z}^* = [360, 360, 360, 360]$  MW, that is, the point forecast is 360



(a) Total downward reserves

(b) Total upward reserves



(c) Violation probability

(d) Expected system operating cost

Figure 1. Medium level of wind penetration,  $N = 100$  and  $\epsilon = 0.1$ : Total downward and upward reserve capacity and performance metrics

MW for all the wind power plants. Hence, the level of wind power penetration in the system (i.e., the ratio of the predicted system-wise wind power production to the total system demand) is approximately 63%.

Figures 1 and 2 illustrate the box plots corresponding to the total downward and upward reserve capacity that is scheduled, the violation probability and the out-of-sample performance delivered by DROTRIMM and PDROW as a function of their respective robustness parameter for sample sizes  $N = 100$  and  $N = 200$ , respectively.

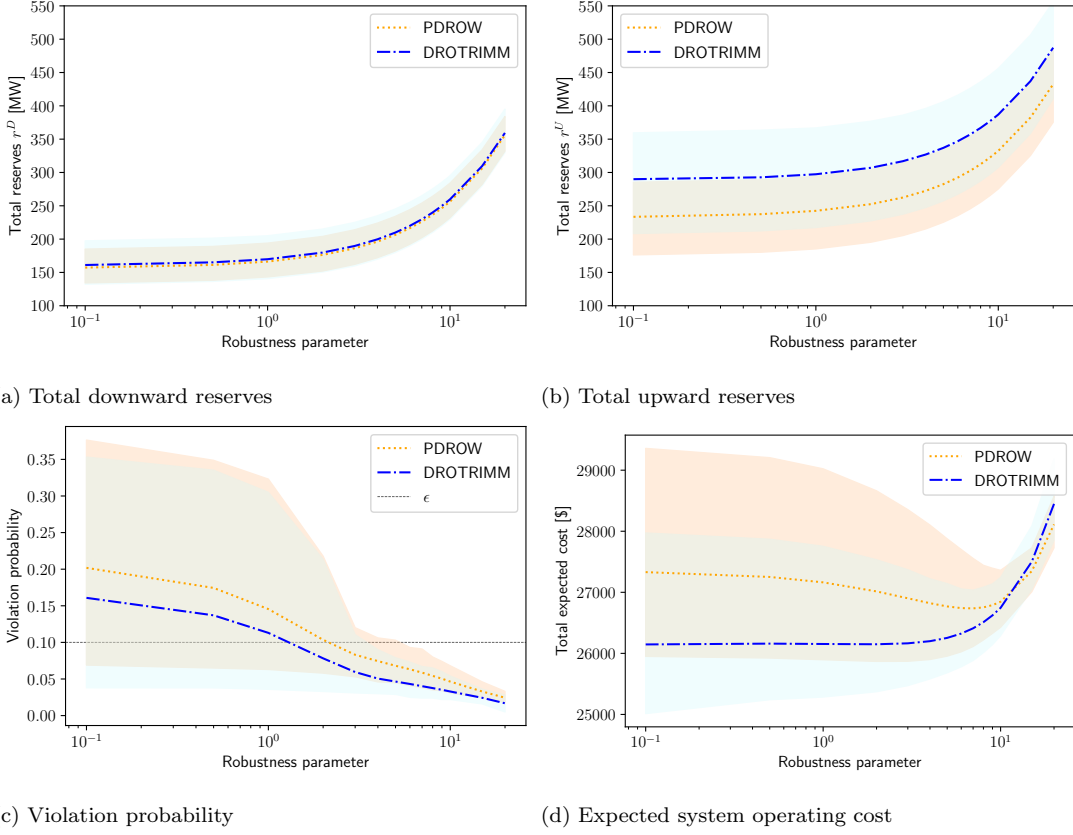


Figure 2. Medium level of wind penetration,  $N = 200$  and  $\epsilon = 0.1$ : Total downward and upward reserve capacity and performance metrics

The box plots have been obtained from 200 independent runs for each sample size. We have set  $\epsilon = 0.1$ . The robustness parameter of PDROW is the radius of the Wasserstein ball, while the robustness parameter for DROTRIMM is the budget excess over the minimum transportation budget (recall Definition 1) [9].

The color-shaded areas have been obtained by joining the 5th and 95th percentiles of the box plots, while the associated bold colored lines link their means. These figures allow us to check which of the methods provides the most cost-efficient dispatch solu-

tions on average without exceeding the threshold  $\epsilon$ . Naturally, the system’s reliability increases as the value of the robustness parameter is augmented, because more reserve capacity is procured. In turn, as more reserve capacity is scheduled, the magnitude and frequency of expensive load shedding events tend to diminish, which explains why the expected system operating cost may also decrease with the robustness parameter. This justifies the use of Distributionally Robust Optimization to tackle the chance-constrained OPF problem. However, when said parameter reaches a large enough value, the expected cost starts to grow quickly, because the cost of procuring additional reserve capacity no longer compensates for the cost savings entailed by the reduction in the amount of curtailed load.

When comparing DROTRIMM and PDROW, the former systematically needs a lower value of the robustness parameter to attain the same level of system reliability. Furthermore, DROTRIMM also identifies dispatch solutions that are systematically cheaper. This phenomenon becomes even more evident when we increase the sample size  $N$  from 100 to 200. A richer joint data sample contains more information on the statistical dependence of the wind power forecast error on the associated point prediction, which our approach manages to take advantage of. To give some numbers, if we just consider the range of values for the robustness parameters for which the violation probability is kept below the tolerance  $\epsilon$ , the relative difference in terms of average out-of-sample performance between DROTRIMM and PDROW goes from 0.37%, when  $N = 100$  to 2.68%, when  $N = 200$ . The difference in performance between the methods is substantially higher if we focus on the 95th percentiles instead. From an engineering point of view, this difference is due to the fact that PDROW underestimates the amount of upward reserve capacity that should be procured, clearly because this method is oblivious to the context.

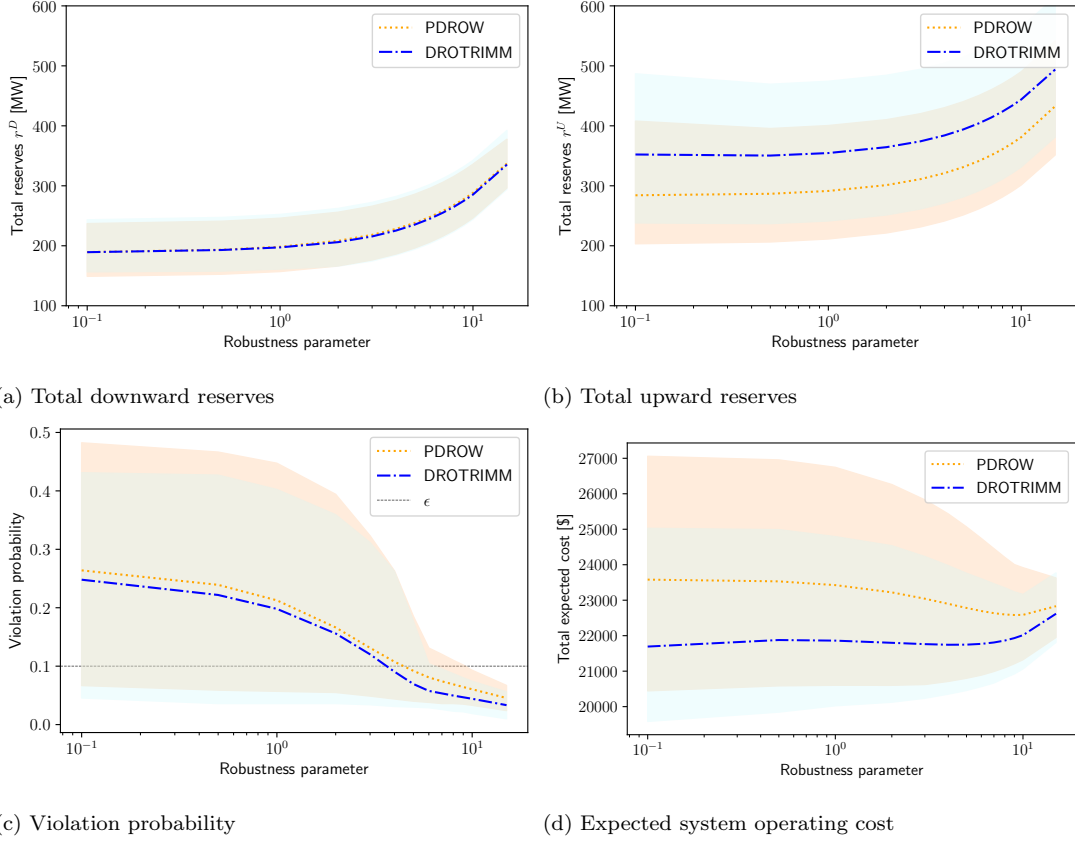


Figure 3. High level of wind penetration,  $N = 100$  and  $\epsilon = 0.1$ : Total downward and upward reserve capacity and performance metrics

### 5.2.2. High wind penetration case

In this alternative setting, all the wind farms have a capacity of 500 MW and the context is given by  $\mathbf{z}^* = [450, 450, 450, 450]$  MW. Hence, the level of wind power penetration in the system is approximately 80%. Figures 3 and 4 are analogous to Figures 1 and 2 of the previous case. The higher level of wind power penetration in this new instance implies a higher level of uncertainty in the system. This accentuates the difference in performance between PDROW and DROTRIMM when  $N = 100$ ,

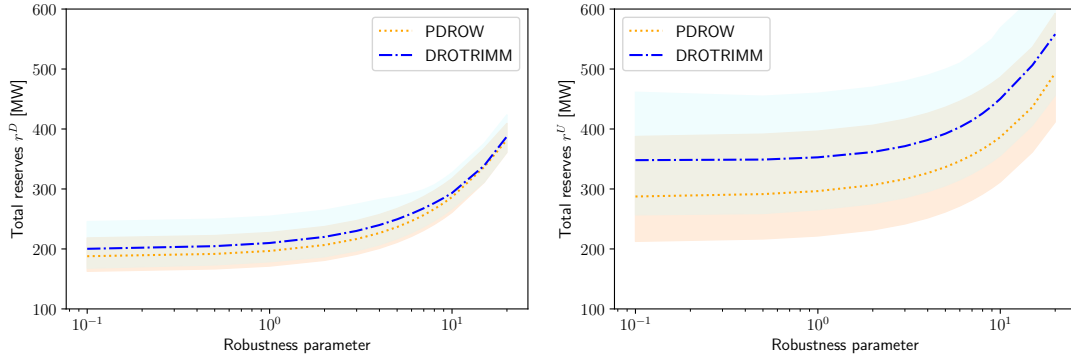
that is, in a small sample regime. More specifically, the relative difference between the out-of-sample average cost achieved by PDROW and DROTRIMM increases from 0.37% in the previous case to 3.67% in this new one. It is also remarkable how small the variance of DROTRIMM is in contrast to that of PDROW, even smaller than in the case of a medium wind power penetration level (compare the range of the box plots in Figure 4). This difference is again caused by the fact that PDROW systematically underestimates the optimal level of reserves.

We conclude this section with a remark on computational time. The continuous linear program that results from tackling the chance-constrained DRO OPF problem by way of DROTRIMM and the CVaR approximation takes around 30 minutes to be solved on average, for a sample size  $N = 200$ , using CPLEX 20.1.0 on a Linux-based server with 6 CPUs clocking at 2.6 GHz and 60 GB of RAM in total.

## 6. Conclusion

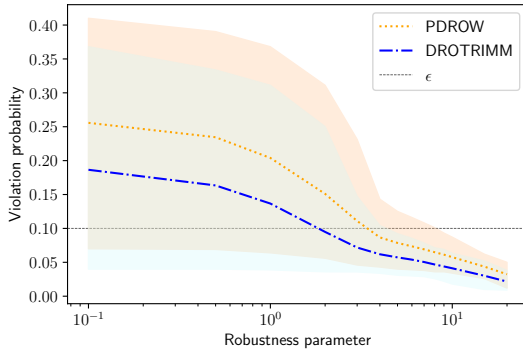
In this paper, we have developed a distributionally robust chance-constrained OPF model that is able to exploit contextual information through an ambiguity set based on probability trimmings. We have provided a reformulation of this model as a continuous linear program using the well-known **CVaR** approximation. By way of a series of numerical experiments conducted on a modified 118-bus power network with wind uncertainty, we have shown that, by exploiting the statistical dependence between the point forecast of the wind power outputs and its associated forecast error, our approach can identify dispatch solutions that, while satisfying the required system reliability, lead to costs savings of up to several percentage points with respect to the OPF solutions provided by an alternative DRO method that ignores said statistical dependence.



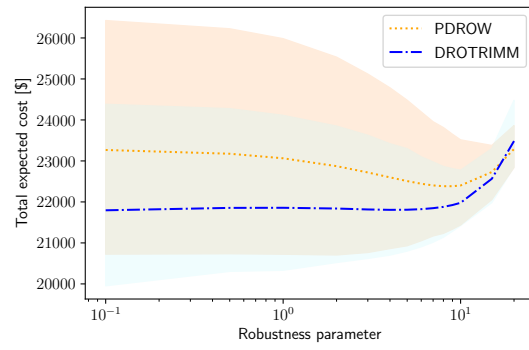


(a) Total downward reserves

(b) Total upward reserves



(c) Violation probability



(d) Expected system operating cost

Figure 4. High level of wind penetration,  $N = 200$  and  $\epsilon = 0.1$ : Total downward and upward reserve capacity and performance metrics

In future work, we plan to devise data-driven schemes for appropriately tuning the robustness parameter in our distributionally robust chance-constrained OPF model in accordance with the risk preferences of the system operator (for instance, by resorting to cross-validation or bootstrapping). We also want to extend this model to account for intertemporal constraints, which, among other things, would involve adapting our probability-trimming-based ambiguity set to deal with stochastic processes and time series data.

### **Acknowledgments**

This work was supported in part by the European Research Council (ERC) under the EU Horizon 2020 research and innovation program (grant agreement No. 755705), in part by the Spanish Ministry of Science and Innovation through project PID2020-115460GB-I00/AEI/10.13039/501100011033, and in part by the Junta de Andalucía (JA) and the European Regional Development Fund (FEDER) through the research project P20\_00153. Finally, the authors thankfully acknowledge the computer resources, technical expertise, and assistance provided by the SCBI (Supercomputing and Bioinformatics) center of the University of Málaga.

### **References**

- [1] Arrigo, A., Kazempour, J., De Grève, Z., Toubreau, J.-F., & Vallée, F. (2021). Embedding dependencies within distributionally robust optimization of modern power systems. *arXiv preprint, arXiv:2104.08101*.
- [2] Arrigo, A., Ordoudis, C., Kazempour, J., De Grève, Z., Toubreau, J.-F., & Vallée, F. (2022). Wasserstein distributionally robust chance-constrained optimization

- for energy and reserve dispatch: An exact and physically-bounded formulation. *Eur. J. Oper. Res.*, 296, 304–322.
- [3] del Barrio, E., & Matrán, C. (2013). Rates of convergence for partial mass problems. *Probab. Theory Relat. Field*, 155, 521–542.
- [4] Bertsimas, D., McCord, C., & Sturt, B. (2019). Dynamic optimization with side information. *arXiv preprint*, *arXiv:1907.07307*.
- [5] Bienstock, D., Chertkov, M., & Harnett, S. (2014). Chance-constrained optimal power flow: Risk-aware network control under uncertainty. *SIAM Rev.*, 56, 461–495.
- [6] Bludszweit, H., Dominguez-Navarro, J., & Llombart, A. (2008). Statistical analysis of wind power forecast error. *IEEE Trans. Power Syst.*, 23, 983–991.
- [7] Chen, Z., Kuhn, D., & Wiesemann, W. (2018). Data-driven chance constrained programs over wasserstein balls. *arXiv preprint*, *arXiv:1809.00210*.
- [8] Duan, C., Fang, W., Jiang, L., Yao, L., & Liu, J. (2018). Distributionally robust chance-constrained approximate AC-OPF with Wasserstein metric. *IEEE Trans. Power Syst.*, 33, 4924–4936.
- [9] Esteban-Pérez, A., & Morales, J. M. (2020). Distributionally robust stochastic programs with side information based on trimmings—Extended version. *arXiv preprint*, *arXiv:2009.10592*.
- [10] Esteban-Pérez, A., & Morales, J. M. (2021). Distributionally Robust Optimal Power Flow with Contextual Information – Codes and Data. *GitHub repository*, [https://github.com/groupoasys/DRO\\_DCOPTF\\_CONTEXTUAL](https://github.com/groupoasys/DRO_DCOPTF_CONTEXTUAL).

- [11] Fabbri, A., Gomez San Roman, T., Rivier Abbad, J., & Mendez Quezada, V. (2005). Assessment of the cost associated with wind generation prediction errors in a liberalized electricity market. *IEEE Trans. Power Syst.*, *20*, 1440–1446.
- [12] Guo, Y., Baker, K., Dall’Anese, E., Hu, Z., & Summers, T. H. (2019). Data-based distributionally robust stochastic optimal power flow—Part I: Methodologies. *IEEE Trans. Power Syst.*, *34*, 1483–1492.
- [13] Hanasusanto, G. A., Roitch, V., Kuhn, D., & Wiesemann, W. (2017). Ambiguous joint chance constraints under mean and dispersion information. *Oper. Res.*, *65*, 751–767.
- [14] Hong, T., Pinson, P., Fan, S., Zareipour, H., Troccoli, A., & Hyndman, R. J. (2016). Probabilistic energy forecasting: Global energy forecasting competition 2014 and beyond. *Int. J. Forecast.*, *32*, 896–913.
- [15] Jabr, R. A. (2020). Distributionally robust CVaR constraints for power flow optimization. *IEEE Trans. Power Syst.*, *35*, 3764–3773.
- [16] Jia, M., Hug, G., & Shen, C. (2021). Iterative decomposition of joint chance constraints in OPF. *IEEE Trans. Power Syst.*, *36*, 4836–4839.
- [17] Li, B., Jiang, R., & Mathieu, J. L. (2016). Distributionally robust risk-constrained optimal power flow using moment and unimodality information. In *2016 IEEE 55th Conf. on Decision and Control (CDC)* (pp. 2425–2430).
- [18] Li, B., Jiang, R., & Mathieu, J. L. (2019). Ambiguous risk constraints with moment and unimodality information. *Math. Program.*, *173*, 151–192.
- [19] Li, B., Jiang, R., & Mathieu, J. L. (2019). Distributionally robust chance-

- constrained optimal power flow assuming unimodal distributions with misspecified modes. *IEEE Trans. Control Netw. Syst.*, *6*, 1223–1234.
- [20] Lubin, M., Dvorkin, Y., & Backhaus, S. (2016). A robust approach to chance constrained optimal power flow with renewable generation. *IEEE Trans. Power Syst.*, *31*, 3840–3849.
- [21] Mieth, R., & Dvorkin, Y. (2018). Data-driven distributionally robust optimal power flow for distribution systems. *IEEE Control Systems Letters*, *2*, 363–368.
- [22] Mohajerin Esfahani, P., & Kuhn, D. (2018). Data-driven distributionally robust optimization using the Wasserstein metric: performance guarantees and tractable reformulations. *Math. Program.*, *171*, 115–166.
- [23] Morales, J. M., Conejo, A. J., Liu, K., & Zhong, J. (2012). Pricing electricity in pools with wind producers. *IEEE Trans. Power Syst.*, *27*, 1366–1376.
- [24] Peña Ordieres, A., Molzahn, D. K., Roald, L. A., & Wächter, A. (2020). DC optimal power flow with joint chance constraints. *IEEE Trans. Power Syst.*, *36*, 147–158.
- [25] Ordoudis, C., Nguyen, V. A., Kuhn, D., & Pinson, P. (2021). Energy and reserve dispatch with distributionally robust joint chance constraints. *Oper. Res. Lett.*, *49*, 291–299.
- [26] Poolla, B. K., Hota, A. R., Bolognani, S., Callaway, D. S., & Cherukuri, A. (2020). Wasserstein distributionally robust look-ahead economic dispatch. *IEEE Trans. Power Syst.*, (pp. 1–1).
- [27] Rahimian, H., & Mehrotra, S. (2019). Distributionally robust optimization: A review. *arXiv preprint, arXiv:1908.05659*.

- [28] Roald, L., Oldewurtel, F., Krause, T., & Andersson, G. (2013). Analytical reformulation of security constrained optimal power flow with probabilistic constraints. In *2013 IEEE Grenoble Conference* (pp. 1–6). IEEE.
- [29] Roald, L., Oldewurtel, F., Van Parys, B., & Andersson, G. (2015). Security constrained optimal power flow with distributionally robust chance constraints. *arXiv preprint arXiv:1508.06061*, .
- [30] Rockafellar, R. T., & Uryasev, S. (2000). Optimization of conditional value-at-risk. *J. Risk*, *2*, 21–41.
- [31] Stott, B., Jardim, J., & Alsac, O. (2009). DC power flow revisited. *IEEE Trans. Power Syst.*, *24*, 1290–1300.
- [32] Vrakopoulou, M., Margellos, K., Lygeros, J., & Andersson, G. (2013). A probabilistic framework for reserve scheduling and  $n - 1$  security assessment of systems with high wind power penetration. *IEEE Trans. Power Syst.*, *28*, 3885–3896.
- [33] Xie, W., & Ahmed, S. (2018). Distributionally robust chance constrained optimal power flow with renewables: A conic reformulation. *IEEE Trans. Power Syst.*, *33*, 1860–1867.
- [34] Xie, W., & Ahmed, S. (2020). Bicriteria approximation of chance-constrained covering problems. *Oper. Res.*, *68*, 516–533.
- [35] Zhang, H., & Li, P. (2011). Chance constrained programming for optimal power flow under uncertainty. *IEEE Trans. Power Syst.*, *26*, 2417–2424.
- [36] Zhou, A., Yang, M., Wang, M., & Zhang, Y. (2020). A linear programming approximation of distributionally robust chance-constrained dispatch with Wasserstein distance. *IEEE Trans. Power Syst.*, *35*, 3366–3377.

## Appendix A. Notation

The main notation used throughout the text is stated below for quick reference. Other symbols are defined as required.

### *Appendix A.1. Sets, Numbers and Indices*

$B$  Set of buses, indexed by  $b$ .

$\mathcal{L}$  Set of lines, indexed by  $\ell$ .

$N_G$  Number of generators (conventional units), indexed by  $j$ .

$N_W$  Number of wind power plants, indexed by  $m$ .

### *Appendix A.2. Parameters and functions*

$f_m$  Forecasted power output at wind power plant  $m$  [MW].

$\tilde{f}_m$  Nominal (p.u.) forecasted power output at wind power plant  $m$ .

$L_b$  Load at bus  $b$  [MW].

$g_j^{\min}, g_j^{\max}$  Upper and lower limit of the power output of generator  $j$  [MW].

$\text{Cap}_\ell$  Capacity of line  $\ell$  [MW].

$\bar{C}_m$  Installed capacity of the wind power plant  $m$  [MW].

$D_\ell$  Row of the matrix  $D$  given by the DC power transfer distribution factors which maps nodal power injections to power flow through line  $\ell$ .

$c_j^D, c_j^U$  Downward and upward reserve procurement cost of generator  $j$  [\$/MW].

$C_j$  Production cost of generator  $j$  given by a piecewise linear function with  $S_j$  pieces/blocks:  $C_j(x) := \max_{s=1, \dots, S_j} \{m_s^j x + n_s^j\}$  where  $m_s^j, n_s^j$  stands for the slope and the intercept of the  $s$ -th piece for generator  $j$ , respectively [\$/].

*Appendix A.3. Random variables and uncertain parameters*

$\boldsymbol{\omega}$	Random vector representing the wind power forecast errors of the $N_W$ wind power plants [MW].
$\Xi_{\boldsymbol{\omega}}$	Support set of the random vector $\boldsymbol{\omega}$ .
$\tilde{\Xi}_{\boldsymbol{\omega}}$	Conditional support set of the random vector $\boldsymbol{\omega}$ .
$\Omega$	Random variable defined as $\sum_{m=1}^{N_W} \omega_m$ , which describes the system-wise aggregate wind power forecast error [MW].
$W_m$	Nominal (p.u.) actual power output at wind power plant $m$ .
$\mathbf{z}$	Random vector representing the features/covariates.
$\Xi$	Support set of the random vector $(\mathbf{z}, \boldsymbol{\omega})$ .
$\tilde{\Xi}$	Side/contextual information.
$\tilde{\Xi}_{\Omega}$	Side information of the random vector $(\mathbf{z}, \Omega)$ .
$g_j(\boldsymbol{\omega})$	Power generation output of generator $j$ (random variable) [MW].
$r_j(\boldsymbol{\omega})$	Reserve deployed by generator $j$ (random variable) [MW].
$\mathbb{E}_Q$	Expectation operator with respect to the probability measure $Q$ .
$\delta_{\xi}$	Dirac distribution at $\xi$ .

*Appendix A.4. Variables*

$g_j$	Power dispatch of generator $j$ [MW].
$\beta_j$	Participation factor of generator $j$ .



- $r_j^D, r_j^U$  Downward and upward reserve capacity provided by generator  $j$  [MW].
- $\mathbf{x}$  Vector of decision variables, that is,  $\mathbf{x} := (\mathbf{g}, \boldsymbol{\beta}, \mathbf{r}^D, \mathbf{r}^U)$ .
- $\mathbf{y}$  Vector of first-stage decision variables (power dispatch and reserve capacity provision), that is,  $\mathbf{y} := (\mathbf{g}, \mathbf{r}^D, \mathbf{r}^U)$ .

*Appendix A.5. Other symbols*

- $(x)^+$  Positive part of  $x$ , i.e.,  $\max\{x, 0\}$ .
- $\lfloor x \rfloor$  Floor function of  $x$ , given by  $\max\{m \in \mathbb{Z} / m \leq x\}$ .
- $\langle \cdot, \cdot \rangle$  Dot product.
- $\mathcal{W}_p$   $p$ -Wasserstein distance.
- $\mathcal{P}_p(\tilde{\Xi})$  The set of all probability distributions supported on  $\tilde{\Xi}$  with finite  $p$ -th moment.
- $\mathcal{R}_{1-\alpha}(P)$  The set of all  $(1 - \alpha)$ -trimmings of the probability distribution  $P$ .
- $S_B$  Support function of a set  $B \subseteq \mathbb{R}^d$ , defined as  $S_B(a) := \sup_{b \in B} \langle a, b \rangle$ .
- $Q - \mathbf{CVaR}_\epsilon(\phi(\xi))$  Conditional Value at Risk at level  $\epsilon \in (0, 1)$  of  $\phi(\xi)$  under the probability measure  $Q$ ; that is, the value  $\inf_{\tau \in \mathbb{R}} \{\tau + \frac{1}{\epsilon} \mathbb{E}_Q[(\phi(\xi) - \tau)^+]\}$ .

**Appendix B. Mathematical definitions related to the ambiguity set based on probability trimmings**

**Definition 2** ( $(1 - \alpha)$ -trimmings, Definition 1.1 from [3]). *Given  $0 \leq \alpha \leq 1$  and probability measures  $P, Q \in \mathbb{R}^d$ , we say that  $Q$  is an  $(1 - \alpha)$ -trimming of  $P$  if  $Q$  is absolutely continuous with respect to  $P$ , and the Radon-Nikodym derivative satisfies*

$\frac{dQ}{dP} \leq \frac{1}{\alpha}$ . The set of all  $(1 - \alpha)$ -trimmings (or trimming set of level  $1 - \alpha$ ) of  $P$  will be denoted by  $\mathcal{R}_{1-\alpha}(P)$ .

**Definition 3** (Minimum transportation budget). *Given  $\alpha > 0$ , the minimum transportation budget, which we denote as  $\underline{\epsilon}_{N\alpha}$ , is the  $p$ -Wasserstein distance between the set of probability distributions  $\mathcal{P}_p(\tilde{\Xi})$  and the  $(1 - \alpha)$ -trimming of the empirical distribution  $\hat{\mathbb{Q}}_N$  that is the closest to that set, that is,*

$$\underline{\epsilon}_{N\alpha} = \left( \frac{1}{N\alpha} \sum_{k=1}^{\lfloor N\alpha \rfloor} \text{dist}(\boldsymbol{\xi}_{k:N}, \tilde{\Xi})^p + \left(1 - \frac{\lfloor N\alpha \rfloor}{N\alpha}\right) \text{dist}(\boldsymbol{\xi}_{\lfloor N\alpha \rfloor:N}, \tilde{\Xi})^p \right)^{\frac{1}{p}} \quad (\text{B.1})$$

where  $\boldsymbol{\xi}_{k:N}$  is the  $k$ -th nearest data point from the sample to set  $\tilde{\Xi}$  and  $\text{dist}(\boldsymbol{\xi}_j, \tilde{\Xi}) := \inf_{\boldsymbol{\xi} \in \tilde{\Xi}} \text{dist}(\boldsymbol{\xi}_j, \boldsymbol{\xi}) = \inf_{\boldsymbol{\xi} \in \tilde{\Xi}} \|\boldsymbol{\xi}_j - \boldsymbol{\xi}\|$ .

### Appendix C. Proof of Proposition 2

Based on [9, Theorem 1], the DRO problem defined by (30) can be reformulated as follows:

$$\inf_{\lambda \geq 0; \bar{\mu}_i, \forall i \leq N; \theta \in \mathbb{R}} \lambda \tilde{\rho} + \theta + \frac{1}{N\alpha} \sum_{i=1}^N \bar{\mu}_i + \sum_{j=1}^{N_G} (c_j^D r_j^D + c_j^U r_j^U) \quad (\text{C.1})$$

$$\text{s.t. } \bar{\mu}_i + \theta + \lambda \|\mathbf{z}^* - \hat{\mathbf{z}}_i\| \geq \sup_{\Omega \in [\underline{\Omega}, \bar{\Omega}]} \left( \sum_{j=1}^{N_G} \max_{s=1, \dots, S_j} \left\{ m_s^j [g_j - \beta_j \Omega] + n_s^j \right\} - \lambda |\Omega - \hat{\Omega}_i| \right), \quad \forall i \leq N \quad (\text{C.2})$$

$$\bar{\mu}_i \geq 0, \quad \forall i \leq N \quad (\text{C.3})$$

Now, constraint (C.2) is equivalent to the following ones:

$$\bar{\mu}_i + \theta + \lambda \|\mathbf{z}^* - \hat{\mathbf{z}}_i\| \geq t_i, \quad \forall i \leq N \quad (\text{C.4})$$

$$t_i \geq \sup_{\Omega \in [\underline{\Omega}, \overline{\Omega}]} \sum_{j=1}^{N_G} \max_{s=1, \dots, S_j} \left\{ m_s^j [g_j - \beta_j \Omega] + n_s^j \right\} - \lambda |\Omega - \widehat{\Omega}_i|, \quad \forall i \leq N \quad (\text{C.5})$$

In order to reformulate the supremum on the right-hand side of (C.5), we resort to the following partition of the set  $\{1, \dots, N\}$ :

$$\underline{I} := \{i \in \{1, \dots, N\} : \widehat{\Omega}_i < \underline{\Omega}\} \quad (\text{C.6})$$

$$I := \{i \in \{1, \dots, N\} : \widehat{\Omega}_i \in [\underline{\Omega}, \overline{\Omega}]\} \quad (\text{C.7})$$

$$\overline{I} := \{i \in \{1, \dots, N\} : \widehat{\Omega}_i > \overline{\Omega}\} \quad (\text{C.8})$$

In this way, because of the convexity of the sum of a maximum of affine functions, constraint (C.5) can be replaced by the following set of constraints:

$$t_i \geq \sum_{j=1}^{N_G} \max_{s=1, \dots, S_j} \left\{ m_s^j [g_j - \beta_j \underline{\Omega}] + n_s^j \right\} - \lambda(\underline{\Omega} - \widehat{\Omega}_i), \quad \forall i \in \underline{I} \quad (\text{C.9})$$

$$t_i \geq \sum_{j=1}^{N_G} \max_{s=1, \dots, S_j} \left\{ m_s^j [g_j - \beta_j \overline{\Omega}] + n_s^j \right\} - \lambda(\overline{\Omega} - \widehat{\Omega}_i), \quad \forall i \in \underline{I} \quad (\text{C.10})$$

$$t_i \geq \sum_{j=1}^{N_G} \max_{s=1, \dots, S_j} \left\{ m_s^j [g_j - \beta_j \underline{\Omega}] + n_s^j \right\} + \lambda(\underline{\Omega} - \widehat{\Omega}_i), \quad \forall i \in \overline{I} \quad (\text{C.11})$$

$$t_i \geq \sum_{j=1}^{N_G} \max_{s=1, \dots, S_j} \left\{ m_s^j [g_j - \beta_j \overline{\Omega}] + n_s^j \right\} + \lambda(\overline{\Omega} - \widehat{\Omega}_i), \quad \forall i \in \overline{I} \quad (\text{C.12})$$

$$t_i \geq \sum_{j=1}^{N_G} \max_{s=1, \dots, S_j} \left\{ m_s^j [g_j - \beta_j \overline{\Omega}] + n_s^j \right\} - \lambda(\overline{\Omega} - \widehat{\Omega}_i), \quad \forall i \in I \quad (\text{C.13})$$

$$t_i \geq \sum_{j=1}^{N_G} \max_{s=1, \dots, S_j} \left\{ m_s^j [g_j - \beta_j \underline{\Omega}] + n_s^j \right\} + \lambda(\underline{\Omega} - \widehat{\Omega}_i), \quad \forall i \in I \quad (\text{C.14})$$

$$t_i \geq \sum_{j=1}^{N_G} \max_{s=1, \dots, S_j} \left\{ m_s^j [g_j - \beta_j \widehat{\Omega}_i] + n_s^j \right\}, \quad \forall i \in I \quad (\text{C.15})$$

Introducing epigraphical auxiliary variables  $\underline{t}_{ij}$ ,  $\overline{t}_{ij}$  and  $\widehat{t}_{ij}$ , we finish the proof.  $\square$ .

## Appendix D. Real-time re-dispatch problem

This appendix contains the optimization program used to evaluate the out-of-sample performance of a given solution of the chance-constrained DC-OPF problem. Given  $N$ , a data-driven solution  $\mathbf{y}_N := (\mathbf{g}, \mathbf{r}^D, \mathbf{r}^U)_N$  and a realization of the forecast error  $\widehat{\boldsymbol{\omega}}_i$ , the operator of the system solves the following deterministic linear program:

$$\min_{\mathbf{r}, \boldsymbol{\Delta d}, \boldsymbol{\Delta \omega}} \sum_{j=1}^{N_G} C_j (g_{j,N} + r_j) + \sum_{b \in B} c_b^{\text{shed}} \Delta d_b + \sum_{j=1}^{N_G} (c_j^D r_j^D + c_j^U r_j^U) \quad (\text{D.1})$$

$$\text{s.t. } \mathbf{0} \leq \boldsymbol{\Delta d} \leq \mathbf{L} \quad (\text{D.2})$$

$$\mathbf{0} \leq \boldsymbol{\Delta \omega} \leq \mathbf{f} + \widehat{\boldsymbol{\omega}}_i \quad (\text{D.3})$$

$$-\mathbf{r}_N^D \leq \mathbf{r} \leq \mathbf{r}_N^U \quad (\text{D.4})$$

$$\sum_{j=1}^{N_G} r_j + \sum_{b \in B} \Delta d_b + \sum_{m=1}^{N_W} (\widehat{\omega}_{i,m} - \Delta \omega_m) = 0 \quad (\text{D.5})$$

$$-\text{Cap}_\ell \leq D_\ell (\mathbf{g}_N + \mathbf{r} + \mathbf{f} + \widehat{\boldsymbol{\omega}}_i - \boldsymbol{\Delta \omega} - \mathbf{L} + \boldsymbol{\Delta d}) \leq \text{Cap}_\ell, \quad \forall \ell \in \mathcal{L} \quad (\text{D.6})$$

where  $\mathbf{r}$ ,  $\boldsymbol{\Delta d}$  and  $\boldsymbol{\Delta \omega}$  are the deployed reserves, load shedding and wind spillage vector of decision variables; and the parameter  $c_b^{\text{shed}}$  is the load shedding cost at bus  $b$ . The objective function in (D.1) minimizes the total operational cost of the system, which comprises the electricity generation cost, the load shedding cost and the total cost of up- and down-reserve capacities. The latter is known and constant and thus, does not intervene in the minimization. Constraints (D.2) and (D.2) limit the amount of load involuntarily curtailed and the amount of wind power unused to the actual realizations of the load and the wind power production, respectively. Constraint (D.4) ensures that the deployed reserves are kept within the reserve capacities scheduled in the forward stage. Constraint (D.5) constitutes the real-time power balance equation and, finally, constraints (D.6) enforce the transmission capacity limits.

## Appendix E. Illustrative example (3-bus system)

In this appendix, we use a small three-node system to illustrate how our DRO framework based on probability trimmings, named DROTRIMM, compares to that proposed in [4], which we refer to as KNNDRO. This other approach is based on a local inference method (specifically, a  $K$ -nearest neighbors), to construct, from the joint data sample, the conditional empirical distribution at which a Wasserstein ball is centered. We also compare DROTRIMM with the PDROW approach introduced in Section 5 of the main text. Actually, PDROW becomes equivalent to KNNDRO when taking  $K = N$ .

The topology of the three-bus system has been taken from [23]. It includes three lines connecting buses 1–2, 2–3, and 1–3, three generators located at nodes 1, 2 and 3, and a 200-MW load connected to bus 3. The production cost of the three generators is modeled as a piecewise function consisting of three pieces. Further details on the generators’ and network’s parameters can be found in Appendix F.

We consider one wind power plant placed at bus 2 with an installed capacity of  $\bar{C}_1 = 60$  MW. Its predicted power output is assumed to be  $z^* = f_1 = 30$  MW in this example. We also assume that the system operator has a series of data pairs given by past point forecasts of the power output at the wind farm and their associated forecast error. Figure E.5 shows a heat map of the true bivariate joint distribution of the forecast power output and its error, together with a kernel estimate of the probability density function of the random forecast error  $\omega$  conditional on  $z^* = 30$  MW. The joint support set  $\Xi$  is polyhedral, and recall that the conditional support varies with the value of  $z$  (see the red line in Figure E.5).

The box plots corresponding to the total downward and upward reserve capacity that is procured, the violation probability and the out-of-sample performance de-

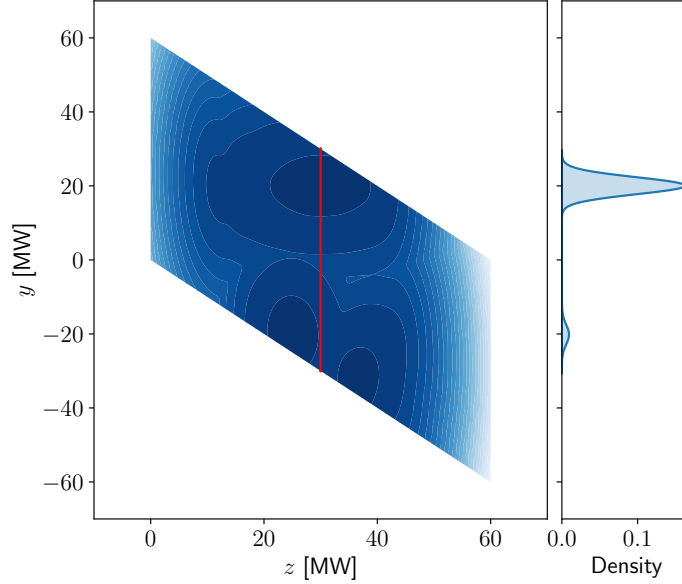


Figure E.5. Heat map of the true joint distribution and kernel estimate of the true conditional density given  $z^* = 30$  MW

livered by each of the considered CC-DRO OPF models is depicted in Figures E.6 and E.7 as a function of their respective robustness parameter, estimated over 200 independent runs for a fixed sample size  $N = 30$  and  $N = 2000$ , respectively. The robustness parameter of KNNDRO and PDROW corresponds to the radius of the Wasserstein ball these methods use as the ambiguity set. For its part, the robustness parameter for DROTRIMM is to be greater than or equal to the minimum transportation budget to the power of  $p$  (we have taken  $p = 1$ , see Definition 1). Therefore, what the system operator really needs to tune in DROTRIMM is the budget excess as done in [9]. This is what we represent in the  $x$ -axes of the aforementioned figures for this method.

As in the case study in Section 5 of the main text, the color-shaded areas have been obtained by joining the *5th* and *95th* percentiles of the box plots, while the associated

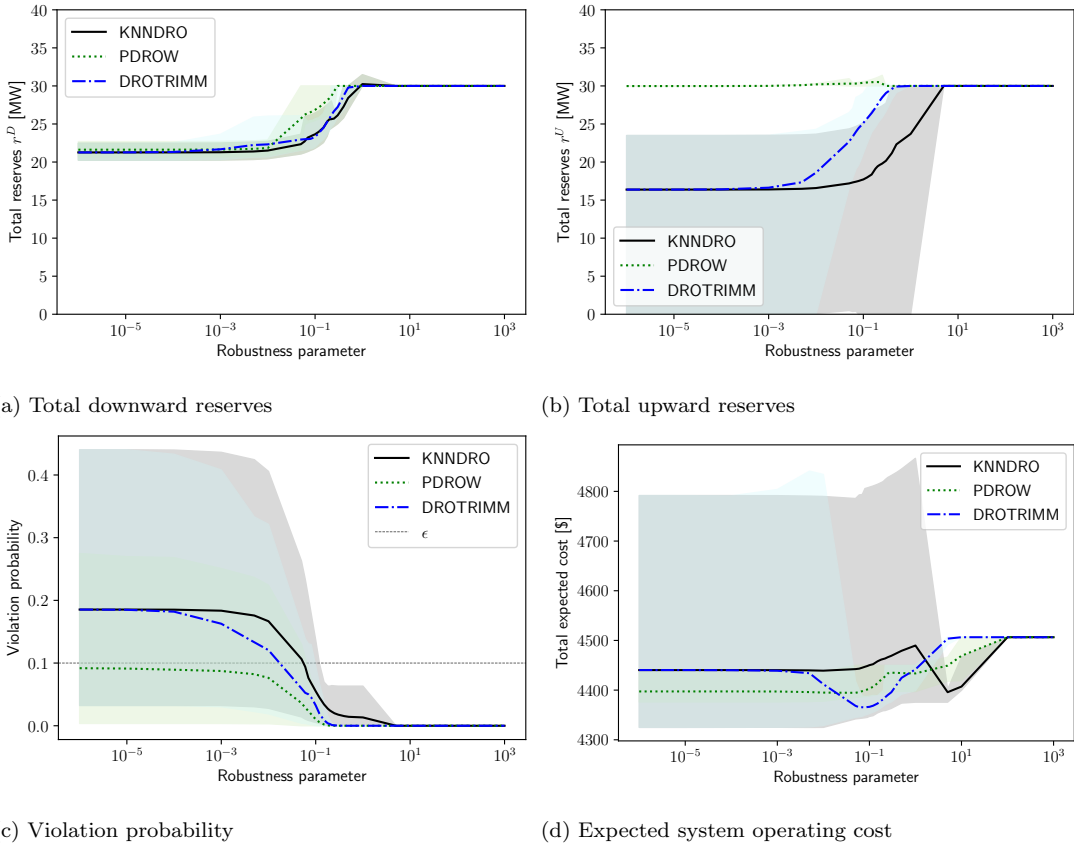


Figure E.6. Three-bus system, sample size  $N = 30$  and  $\epsilon = 0.1$ : Total downward and upward reserves and performance metrics

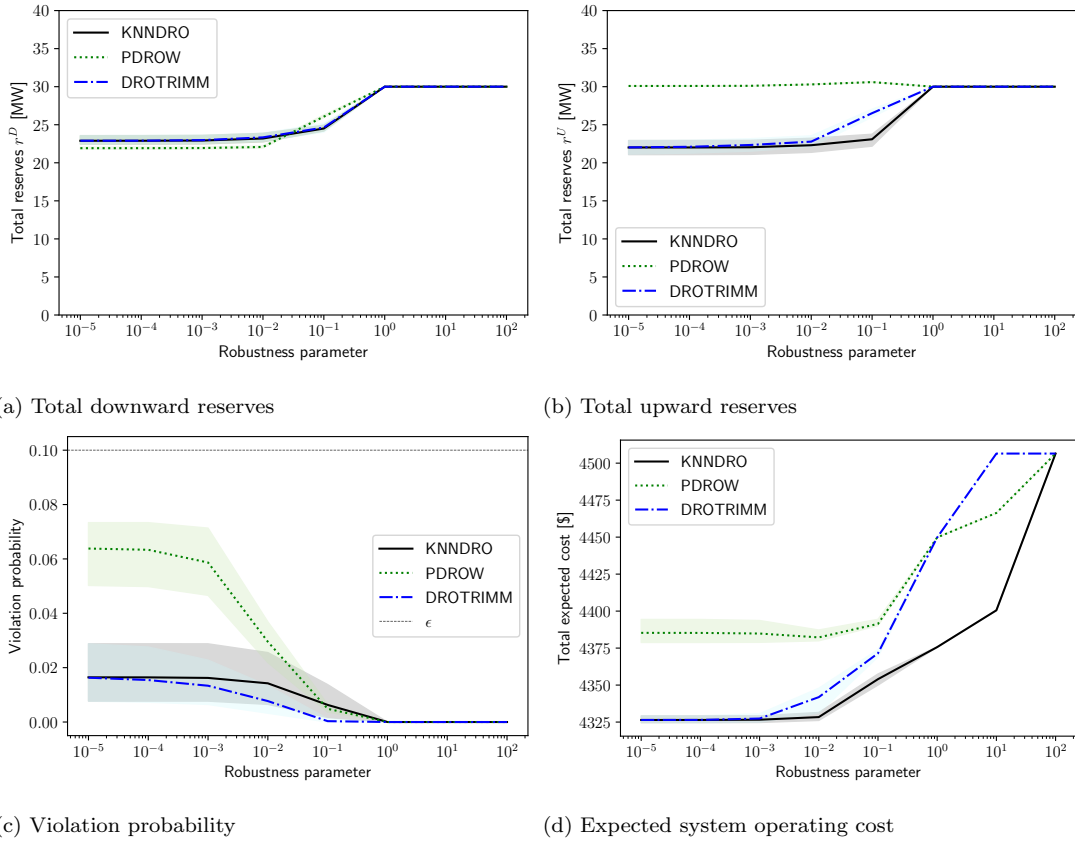


Figure E.7. Three-bus system, sample size  $N = 2000$  and  $\epsilon = 0.1$ : Total downward and upward reserves and performance metrics



bold colored lines link their means. The number of neighbors  $K_N$  we have considered for KNNDR0 is given by the logarithmic rule, that is, if  $N$  is the sample size of the joint data, then the number of neighbors is computed as  $K_N = \lfloor N/(\log(N + 1)) \rfloor$ . To ensure a fair comparison, we have also taken  $\alpha_N = K_N/N$  for DROTRIMM. Figures E.6 and E.7 provide information on the ability of each method to discover good dispatch solutions, that is, scheduling plans for power production and reserve capacity provision that are cost-efficient in expectation while guaranteeing the desired system reliability. We consider two settings, namely, the case of a small sample size, for which the available joint data is expected to carry little information on the true conditional distribution of the wind power forecast error (Figure E.6), and another one where the sample size is notably higher (Figure E.7).

Figure E.6 shows that, for a value of the robustness parameter equal to  $10^3$ , all the methods recover the *robust* dispatch, that is, the dispatch that performs the best under the worst-case value of the forecast error, having predicted 30 MW of wind power production. Additionally, note that DROTRIMM achieves a violation probability that is always lower than or equal to that attained by KNNDR0. Moreover, if we consider values of the robustness parameter smaller than  $10^{-1}$  in Figure E.6c, many of dispatch solutions delivered by DROTRIMM and KNNDR0 lead to a violation probability higher than the threshold  $\epsilon = 0.1$ , which highlights the value of *distributional robustness* in the OPF problem under uncertainty.

When  $N = 30$ , PDROW exhibits a nice behavior both in terms of out-of-sample expected system operating cost and system reliability. However, like DROTRIMM, this method also needs a value of its robustness parameter around  $10^{-1}$  (or greater) to ensure that almost none of the dispatch solutions it provides violate the reliability threshold  $\epsilon = 0.1$ . Within a neighborhood of that value, though, DROTRIMM is able to identify dispatch solutions that are about 1% cheaper than those given by PDROW.

Furthermore, DROTRIMM’s solutions are also more cost-efficient on average (and even more reliable) than those of KNNDRO. The reason for this is that KNNDRO does not explicitly protect the dispatch against the potential conditional inference error incurred by the local predictive method it relies on.

When the sample size is high enough, e.g.,  $N = 2000$ , Figure E.7c shows that all the methods provide reliable dispatch solutions (i.e., power dispatches that ensure the threshold  $\epsilon = 0.1$ ) for any value of their respective robustness parameter. However, the solutions given by PDROW are more expensive, because this method procures more upward reserve capacity than needed (see Figure E.7b). On the other hand, the performance of DROTRIMM and KNNDRO tends to be similar in a large-sample regime. Indeed, both are able to disclose dispatches that result in similar system operating costs while guaranteeing the reliability of the system (see Figures E.7c and E.7d in the range of the robustness parameter between  $10^{-5}$  y  $10^{-3}$ ).

As, in our numerical experiments, we have detected that DROTRIMM always provide dispatches with a performance similar or superior to those given by KNNDRO, in the case study of Section 5, we have not discussed the latter.

## **Appendix F. Data for the illustrative example (3-bus system)**

This appendix compiles data pertaining to the illustrative example that has been presented and discussed in Appendix E.

Generator index	Bus index	$c_j^D$	$c_j^U$	$g_j^{\min}$	$g_j^{\max}$
1	1	6	3	0	120
2	2	2	5	0	80
3	3	4	8	0	100

Table F.1. Generators' cost parameters

Generator index	Slopes $m_s$			Intercepts $n_s$		
	piece 1	piece 2	piece 3	piece 1	piece 2	piece 3
1	22	26	30	0	-173	-493
2	29	37	45	0	-231	-658
3	38	55	71	0	-601	-1715

Table F.2. Slopes ( $m_s$ ) and intercepts ( $n_s$ ) of the generators' piecewise linear cost functions

index	from bus	to bus	X (reactance p.u.)	Cap (MW)
1	1	2	0.13	100
2	1	3	0.13	100
3	2	3	0.13	100

Table F.3. Transmission line parameters